



## Insights into adhesion of abalone: A mechanical approach



Jing Li<sup>a</sup>, Yun Zhang<sup>b</sup>, Sai Liu<sup>b</sup>, Jianlin Liu<sup>b,\*</sup>

<sup>a</sup> College of Mechanical and Electrical Engineering, China University of Petroleum (East China), Qingdao 266580, China

<sup>b</sup> College of Pipeline and Civil Engineering, China University of Petroleum (East China), Qingdao 266580, China

### ARTICLE INFO

#### Keywords:

Abalone  
Normal adhesion strength  
Shear adhesion strength  
Capillary force  
Van der Waals force

### ABSTRACT

Many living creatures possess extremely strong capability of adhesion, which has aroused great attention of many scientists and engineers. Based on the self-developed equipment, we measured the normal and shear adhesion strength of the abalone underwater and out of water on different contact surfaces. It is found that the adhesion force of the abalone can amount to 200 or 300 times its body weight. The effects of wettability and roughness of the surface, and the frictional coefficient of mucus on the adhesion strength have been discussed. The theoretical calculation manifests that the normal adhesion force mainly stems from the suction pressure, van der Waals force and capillary force of the pedal, and their limit values are given. These findings may provide some inspirations to engineer new-typed materials, micro-devices, adhesives and medicine.

### 1. Introduction

With evolution in nature millions of years, many living creatures have mastered magic skills to adapt the environment and survive to date. One typical phenomenon is that a plethora of animals have formed the strong capability of adhering to various surfaces. For example, mosquitoes (Wu et al., 2007) and water striders (Hu and Bush, 2010) can stably stay on water surfaces even in the stormy and windy days, as the surface tension can provide a large adhesion force. Another animal is the gecko, and as is well known, it can freely climb on walls or ceilings, which is owing to the van der Waals force between the nanometered fibers on feet and the contact surface (Autumn et al., 2002; Sun et al., 2005; Stark et al., 2016; Klittich et al., 2017). In addition, the tree frogs (Barnes et al., 2006; Federle et al., 2006), and some insects (Langer et al., 2004; Eisner and Aneshansley, 2000), such as ants, flies and mayfly larvae (Ditsche-Kuru et al., 2010) can all attach to solid surfaces because of adhesion. These behaviors have spurred the admiration to uncover the secret of adhesion on these creatures, which has become a hot topic in such areas as material science, micro/nano-devices design, cybernetics, medicine, physics and mechanics. It has been declared that the mechanisms of adhesion for the terrestrial animals may originate from several factors, i.e., the van der Waals force, capillary force, viscous force (or Stefan adhesion), mechanical interlocking, glue through chemical bonding, friction and suction (Ditsche and Summers, 2014).

Despite the growing knowledge of adhesion in terrestrial animals, reasons for that of underwater creatures have not been comprehensively addressed. It is claimed that adhesion occurring underwater is

very complicated, as water can greatly affect the contact interfaces and weaken many forms of bonds (Ditsche and Summers, 2014; Tadmor et al., 2017). Waite (Waite, 1987) mentioned that aquatic animals often adopt some strategies to fulfill underwater adhesion, such as mechanical interlocking, suction and gluing. For instance, the pressure difference provided by suckers both in marine and freshwater systems is a widely used skill, which has been learned by octopi, clingfish and river loach (Tramacere et al., 2013; Wainwright et al., 2013; Chuang et al., 2017). Besides this performance, glue is another common attachment mechanism for some marine animals. It can be seen that mussels and barnacles demonstrate the permanent adhesion by producing quick-acting protein-based glues (Raman et al., 2013; Waite, 2017). Moreover, sandcastle worms build tubular shells under seawater by gluing sand grains and biomineral particles together, in use of a multi-component, rapid-set, and self-initiating adhesive (Zhao et al., 2016; Stewart et al., 2017).

Although much effort has been made on the adhesion of above mentioned animals, there are rarely reports on that of abalone. In practice, abalone belongs to a kind of snail, which has a broad and muscular foot; and this pedal foot enables it to cling solidly to slippery rocky surfaces with high strength at sublittoral depths. The abalone adhesion will greatly affect the energy cost when they adhere to the warships, boats and platforms, which is a serious problem to be solved. Recently, Lin et al. (Lin et al., 2009) measured the adhesion force of the setae distributed on the pedal foot based on AFM (atomic force microscope), and then gave calculations based on the theoretical model. However, there still remain some unsolved questions on the abalone adhesion, such as the adhesion force out of water, the comparison

\* Corresponding author.

E-mail address: [liujianlin@upc.edu.cn](mailto:liujianlin@upc.edu.cn) (J. Liu).

between the normal and shear force, it should be noticed that the peeling of abalone is normally close to the shearing direction in reality. In addition, what the real role of each origin of the adhesion force plays needs to be clarified. Such issues have motivated our inspiration directed towards a comprehensive study on the abalone adhesion.

The outline of this article is organized as follows. Firstly, we introduce the experiment of measuring the normal and shear adhesion strength on the basis of a self-developed mechanical approach. Next, we report that the abalone possess a very huge adhesion capability, and then fully discuss the values of normal and shear adhesion strength, when the abalone underwater or out of water on different contact surfaces. Then we make some mechanics analyses and give the quantitative results of the adhesion force, which are consistent with the experiments. We hope this exploration paves a further step on the adhesion of some special marine organisms.

## 2. Materials and methods

### 2.1. Sample preparation

The abalone used in the experiment is *Haliotis discus hannai*, stemming from coastal areas (Yellow Sea area) of Qingdao city in China. The adult abalones are kept together in a transparent cuboid aquarium with the volume of  $80 \times 60 \times 100 \text{ cm}^3$ , and it is equipped with an air pump, a thermostat ( $18 \pm 1 \text{ }^\circ\text{C}$ ) and a filtration system. After captured, the abalones are fed with algae on a daily basis, within the period of two months. For most of the time, the abalones are statically adhered to the bottom surface or aquarium walls, and only occasionally, they move to a different location when stimulated. Each abalone is 3 years old and about 7 cm in body length. The weight of the abalone is in the range of 61–68 g, with the pedal foot areas ranging from 21.3 to 25.6  $\text{cm}^2$ . All the experiments are conducted after the abalones have been captured for at least 3 days, to ensure they have already adapted the new environment. When taken out of water, the body of abalone is kept physically stimulated to produce mucus secreted from the foot, and a layer of mucus can be collected on the substrate.

### 2.2. Imaging

Next, the image of ventral side of each abalone is captured by a camera (Nikkon D7200), and its adhesive area is then calculated by the software ImageJ (National Institutes of Health). More accurately, the microstructures of the pedal foot are then observed through SEM (scanning electron microscopy, COXEM EM-30 Plus). The alive abalone is anesthetized by immersion in the seawater, where 5%  $\text{MgCl}_2$  is dissolved in it. Then the foot is sectioned from its body and rinsed with ultrapure water from 3 to 5 times. After kept in 10% formaldehyde for at least 48 h, the specimen is dehydrated gradually with 50%, 60%, 85%, 90%, 100% ethanol to prevent its deformation and shrinkage. Finally, the specimen is placed at shady places to dry naturally, and then is cut into several small pieces. Before observation through SEM, the specimens are sputter coated with a thin layer of platinum to enhance the electron conductivity on the surface.

The macroscopic morphology of a pedal foot of abalone (*Haliotis discus hannai*) is photographed by the camera, as shown in Fig. 1(a). Fig. 1(b) and (c) are the high-magnification SEM images of the foot, where a large number of micrometer-scaled fibers are uniaxially aligned, perpendicular to the plane of the foot tissue, and it can be observed that there is some mucus on the fibers. When most of the mucus is removed, the fibers become clearer, and their average diameter is around 1  $\mu\text{m}$ , which is close to that of the adhesive setae of geckos.

### 2.3. Wettability and morphologies of substrates

The wettability of different substrates is characterized with its

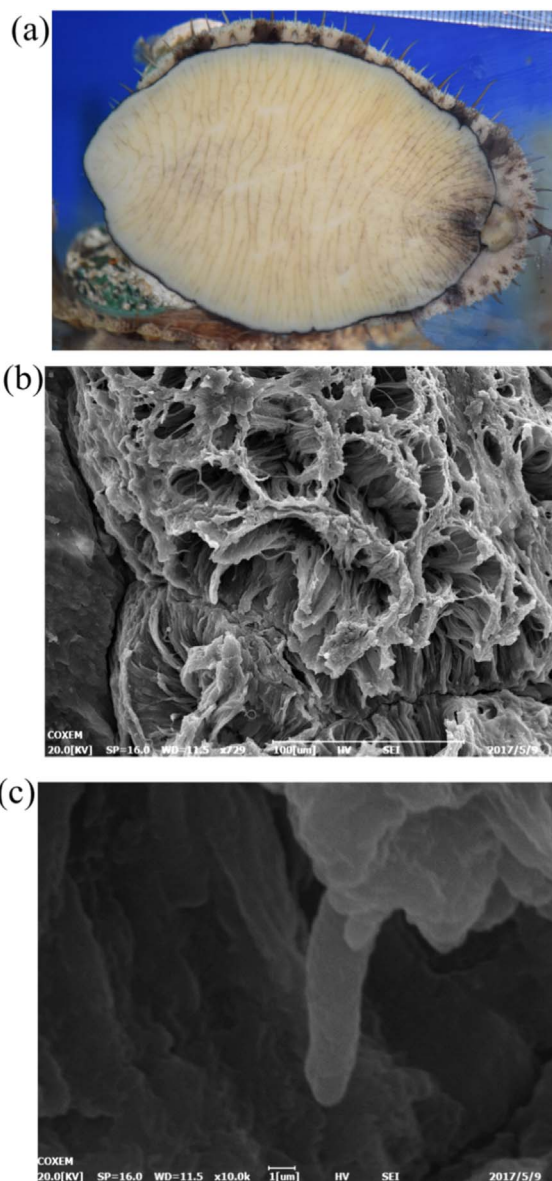


Fig. 1. Images of the abalone's pedal foot. (a) Top view of a pedal foot. (b) SEM image of fibers on the pedal foot. (c) High-magnification SEM image of one fibril, with the diameter around 1  $\mu\text{m}$ .

Young's contact angle, which is measured in use of the contact angle goniometer (Biolin Scientific Corporation, Thetalit 100). In performing the measurement process, a seawater droplet with the volume of  $\sim 2 \mu\text{L}$  is ejected from a dispensing needle, and is gently deposited on the top of the substrate surface. The profile shape of the droplet is fitted using the Young-Laplace equation, and the Young's contact angle of the droplet is obtained via the software on the drop shape analysis. The Young's contact angles of liquid on four substrates, i.e. glass, acrylic, steel and PTFE surfaces are given as  $\theta_Y = 49.89 \pm 2.85^\circ$ ,  $85.08 \pm 2.28^\circ$ ,  $100.32 \pm 1.81^\circ$  and  $123.09 \pm 2.44^\circ$ , respectively. The surface morphology of the substrate is observed using a three-dimensional white light interference surface topography instrument (ZYGONexView). Thus in the  $O$ -xyz coordinate, the roughness information is denoted by the area roughness parameter  $S_a$ , which is defined as

$$S_a = \frac{1}{MN} \sum_{i=1}^M \sum_{j=1}^N |z(x_i, y_j)| \quad (1)$$

where  $M$  and  $N$  are the numbers of data points along  $x$  and  $y$  axis on the

Download English Version:

<https://daneshyari.com/en/article/5020362>

Download Persian Version:

<https://daneshyari.com/article/5020362>

[Daneshyari.com](https://daneshyari.com)